Formation of Silicalite-1 Hollow Spheres by the Self-assembly of Nanocrystals

ARTICLE *in* CHEMISTRY OF MATERIALS · JANUARY 2003

Impact Factor: 8.35 · DOI: 10.1021/cm020786v

4 AUTHORS, INCLUDING:

Sajo P. Naik
Oil Dri Corporation of America
41 PUBLICATIONS **773** CITATIONS
SEE PROFILE

Anthony Shiaw-Tseh Chiang
National Central University
106 PUBLICATIONS **1,603** CITATIONS
SEE PROFILE

Formation of Silicalite-1 Hollow Spheres by the Self-assembly of Nanocrystals

S. P. Naik,[†] A. S. T. Chiang,*[,†] R. W. Thompson,[§] and F. C. Huang[‡]

Department of Chemical and Materials Engineering, and Graduate Institute of Environment Engineering, National Central University, Chung-Li, Taiwan, Republic of China 320, and Department of Chemical Engineering, Worcester Polytechnic Institute, Worcester, Massachusetts 01609

Received July 29, 2002. Revised Manuscript Received October 28, 2002

A simple approach is reported for the preparation of hollow spheres with a 10−20-nm-thick shell of silicalite-1 nanocrystals. The nanocrystals were produced by the steaming of silicalite-1 nanoprecursors (NPs), collected with the help of surfactant from a clear synthesis solution immediately following the induction period. The nanocrystals produced were ≈10−20 nm with a BET surface area of 440−470 m^2/g and an external surface area >112 m^2/g. A water adsorption isotherm confirmed that the nanocrystals were hydrophobic in nature. These nanocrystals self-assembled into hollow spheres of 100−300-nm diameter when ultrasonicated in ammoniac ethanol.

Introduction

One of the keys to realizing nanotechnology is the ability to assemble nanoparticles into three-dimensional (3D) objects. Hollow spheres of submicrometer to micrometer size with controlled porosity in its shell is an object of interest that may lead to applications such as controlled release capsules, artificial cells, chemical sensors, shape-selective catalysts, and adsorbents. Various methods, including cosurfactant,[1,2] phase separation,[3] rapid quench,[4] and ultrasonication,[5] have been reported for the preparation of hollow spheres with mesoporous shells. Hollow spheres of microporous zeolites prepared by the layer-by-layer accumulation of zeolite nanocrystals on polystyrene spheres[6,7] or by the sonication of nanocrystals with toluene-dispersed water droplets[8] have also been reported. Since the smallest zeolite nanocrystals available to date are about 40 nm, the hollow zeolite spheres reported by the above authors were in the micrometer-size range. The size of the hollow spheres could be reduced if smaller zeolite crystals could be prepared.

Microspheres of about 0.5 mm comprised of zeolites were prepared with ion-exchange resins as macrotemplates.[9,10] This led to a structure with zeolitic micropores and large (≈40 nm) mesopores. Zeolite/mesoporous molecular sieve composites were also produced by partial dissolution of the zeolites in NaOH solutions containing surfactants.[11] However, it is not clear whether the ordered mesoporous material walls were comprised of the zeolite crystals themselves, crystal fragments, or purely amorphous aluminosilicates.

In addition to serving as building units for spherical particle assembly, small zeolite nanocrystals may have other applications as well. Less than 10-nm zeolite nanocrystals would have approximately 300 m^2/g of external surface area, comparable to the micropore surface area of typical zeolites measured by the BET method. This external surface area is zeolitic in nature, is accessible to larger molecules, and may be of importance in catalysis and adsorption. For example, it has been demonstrated[12] that the reduction of H−ZSM-5 crystals from 5 μm to 300 nm led to a substantial increase of conversion and selectivity in the isomerization of 2,7-dimethylnaphthalene. Nano-H−ZSM-5 about 60 nm in size has also been found as a promising catalyst in the cracking of polyolefins.[13]

Recently, we[14] reported a new method for producing zeolite nanocrystals smaller than 30 nm. The method involves the isolation of the nanometer-sized zeolitic precursors, hereinafter referred to as nanoprecursors

* To whom correspondence should be addressed. E-mail: stchiang@cc.ncu.edu.tw.

[†] Department of Chemical and Materials Engineering, National Central University.

[‡] Graduate Institute of Environment Engineering, National Central University.

[§] Worcester Polytechnic Institute.

(1) Lin, H. P.; Cheng, Y. R.; Mou, C. Y. *Chem. Mater.* **1998**, *10* (12), 3772−3776.

(2) Lin, H. P.; Mou, C. Y.; Liu, S. B.; Tang, C. Y. *Chem. Commun.* **2001**, *19*, 1970−1971.

(3) Schacht, S.; Huo, Q.; VoigtMartin, I. G.; Stucky, G. D.; Schuth, F. *Science* **1996**, *273* (5276), 768−771.

(4) Fowler, C. E.; Khushalani, D.; Mann, S. *Chem. Commun.* **2001**, *19*, 2028−2029.

(5) Prouzet, E.; Cot F.; Boissiere, C.; Kooyman, P. J.; Larbot, A. *J. Mater. Chem.* **2002**, *12*, 1553−1556.

(6) Wang, X. D.; Yang, W. L.; Tang, Y.; Wang, Y. J.; Fu, S. K.; Gao, Z. *Chem. Commun.* **2000**, *21*, 2161−2162.

(7) Rhodes, K. H.; Davis, S. A.; Caruso, F.; Zhang, B.; Mann, S. *Chem. Mater.* **2000**, *12*, 2832−2834.

(8) Kulak, A.; Lee, Y. J.; Park, Y. S.; Kim, H. S.; Lee, G. S.; Yoon, K. B. *Adv. Mater.* **2002**, *14*, 526−529.

(9) Tosheva, L.; Valtchev, V.; Sterte, J. *Microporous Mesoporous Mater.* **2000**, *35*−*36*, 621−629.

(10) Tosheva, L.; Mihailova, B.; Valtchev, V.; Sterte, J. *Microporous Mesoporous Mater.* **2000**, *39*, 91−101

(11) Goto, Y.; Fukushima, Y.; Ratu, P.; Imada, Y.; Kubota, Y.; Sugi, Y.; Ogura, M.; Matsukata, M. *J. Porous Mater.* **2002**, *9*, 43−48.

(12) Pu, S. B.; Inui, T. *Zeolites* **1996**, *17* (4), 334−339.

(13) Aguado, J.; Serrano, D. P.; Sotelo, J. L.; Van Grieken, R.; Escola, J. M. *Ind. Eng. Chem. Res.* **2001**, *40* (24), 5696−5704.

(14) Naik, S. P.; Chen, J. C.; Chiang, A. S. T. *Microporous Mesoporous Mater.* **2002**, *54*, 293−303.

10.1021/cm020786v CCC: $25.00
Published on Web 01/16/2003

(NPs), and their conversion to nanocrystals by steaming. We now have further improved the synthesis scheme so that the nanocrystal size is reduced to 10−20 nm. When the so-obtained nanocrystals were dispersed and sonicated in ammoniac ethanol, the nanocrystals were found to self-assemble into hollow spheres.

Experimental Section

Synthesis. The NPs of TPA−silicalite-1 were prepared[14,15] as follows: 11.5738 g of TEOS (tetraethoxysilane >98%, Merck) was transferred to a PP (polypropylene) bottle containing 14.1229 g of TPAOH (tetrapropylammonium hydroxide, 20% aq. Merck) and 68 g of DI water. The resulting solution was stirred vigorously at room temperature for about 45 min to hydrolyze TEOS so that a single-phase clear solution was formed. The molar composition of the resulting sol was 0.25/1/80 TPAOH/TEOS/H_2O. This sol was then heated at 80 °C in a tightly capped PP bottle in an air oven. The PP bottle was removed from the oven after 18 h and cooled to room temperature.

Harvesting the NPs. The NPs contained in the sol were then flocculated by slow addition, with stirring, of a surfactant solution of 1.0125 g of CTAMeBr (cetyltrimethylammonium bromide, Aldrich, 99.9%) in 54.2732 g of ethanol (98%, Merck). The stirring was continued for 3 h. The white precipitate was collected by filtration, washed with 300 mL of ethanol, and dried, initially at room temperature for 24 h, and then at 70 °C for 3 h. The dried NPs were pressed into pellets and placed on top of a ceramic honeycomb in a 190-mL stainless steel autoclave with 0.19 g of water at the bottom for steaming. The volume of the ceramic honeycomb was about 12 mL, while the sample occupied <1-mL volume. The steaming step, which was carried out at 150 °C for 24 h, converted the NPs into TPA−silicalite-1 nanocrystals. The nanocrystal zeolite pellets obtained were heated to 300 °C at 5 °C/min and then at 1 °C/min to 550 °C and held at 550 °C for 5 h in a muffle furnace. A reference TPA−silicalite-1 colloid was also prepared from the same composition by extending the 80 °C hydrothermal reaction to 30 h.

Characterization. XRD (X-ray powder diffraction) was carried out on a Shimadzu LAB-X-700 diffractometer using Cu Kα radiation. IR absorption spectra were measured using the KBr wafer technique in a Jasco-410 FTIR instrument. The spectra were recorded with a resolution of 2 cm^{-1} and corrected for background. The microstructure observation was made on a JEOL JEM-200FXII transmission electron microscope (TEM). Nitrogen adsorption measurements were carried out at −196 °C on a Micromeritics ASAP 2010 instrument, whereas the room temperature adsorption of water and *n*-hexane were measured gravimetrically with a G-Cahn-200 microbalance. The calcined samples were activated at 350 °C and <0.1-Pa vacuum before adsorption.

Results and Discussion

NPs Collected. In our previous study,[14] where the hydrothermal reaction was carried out at 100 °C, the introduction of the surfactant/ethanol mixture midway through the reaction was used as a means to prolong the induction period. However, according to Li et al.,[16,17] the induction period can also be increased if the reaction is conducted at a lower temperature, which also leads to a larger population of smaller colloidal zeolite. Since the low-temperature synthesis seemed to be a more direct approach, we chose to reduce the reaction temperature from 100 to 80 °C in this study, instead of using additives.

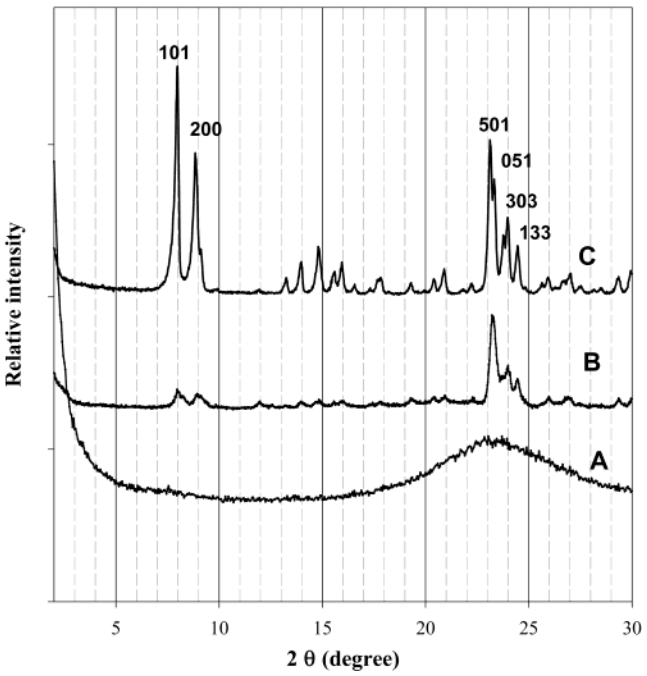

Figure 1. XRD patterns of (A) NPs collected from the clear sol (B) nanocrystals produced after steaming (C) calcined nanocrystals.

Before the preparation of NPs, the growth curve of colloidal silicalite from the same recipe had been monitored by dynamic light scattering (ZetaSizer-3000 from Malvern Instrument Co. with a 10-mW He−Ne laser). It was determined that the batch composition produced discrete colloidal crystals of final size 140 nm after 30 h of hydrothermal reaction at 80 °C. The extrapolation of the growth curve suggested an induction period of about 18 h prior to the onset of crystal growth.

As was demonstrated in our previous study,[14] the materials isolated from the reaction sol right after the induction period consisted of only nanosized precursors. A number of authors have reported similar findings.[18,19] Van Grieken et al.,[20] in their studies of H−ZSM-5 nanocrystals, also reported the formation of seemingly X-ray amorphous pseudocrystalline solid prior to its "zeolitization".

The NPs in the still transparent sol can be effectively collected by the addition of ethanolic CTAMeBr solution. The as-isolated NPs produced a broad band in the XRD pattern consistent with that of nanometer-sized MFI crystallites,[21] as shown in Figure 1A. This broad band was predicted to result from the broadening of the 12 distinct peaks in the 22.5−25.5° 2θ range and should be apparent if there is sufficient concentration of the

(15) Tsay, C. S.; Chiang, A. S. T. *Microporous Mesoporous Mater.* **1998**, *26* (1−3), 89−99.
(16) Li, Q. H.; Creaser, D.; Sterte, J. *Microporous Mesoporous Mater.* **1999**, *31* (1−2), 141−150.
(17) Li, Q. H.; Mihailova, B.; Creaser, D.; Sterte, J. *Microporous Mesoporous Mater.* **2001**, *43* (1), 51−59.
(18) de Moor, P. P. E. A.; Beelen, T. P. M.; van Santen, R. A. *J. Phys. Chem. B* **1999**, *103* (10), 1639−1650.
(19) Kirschhock, C. E. A.; Buschmann, V.; Kremer, S.; Ravishankar, R.; Houssin, C. J. Y.; Mojet, B. L.; van Santen, R. A.; Grobet, P. J.; Jacobs, P. A.; Martens, J. A. *Angew. Chem., Int. Ed.* **2001**, *40* (14), 2637−2640.
(20) Van Grieken, R.; Sotelo J. L.; Menendez, J. M.; Melero, J. A. *Microporous Mesoporous Mater.* **2000**, *39*, 135−147.
(21) Schlenker, J. L.; Peterson, B. K. *J. Appl. Crystallogr.* **1996**, *29*, 178−185.

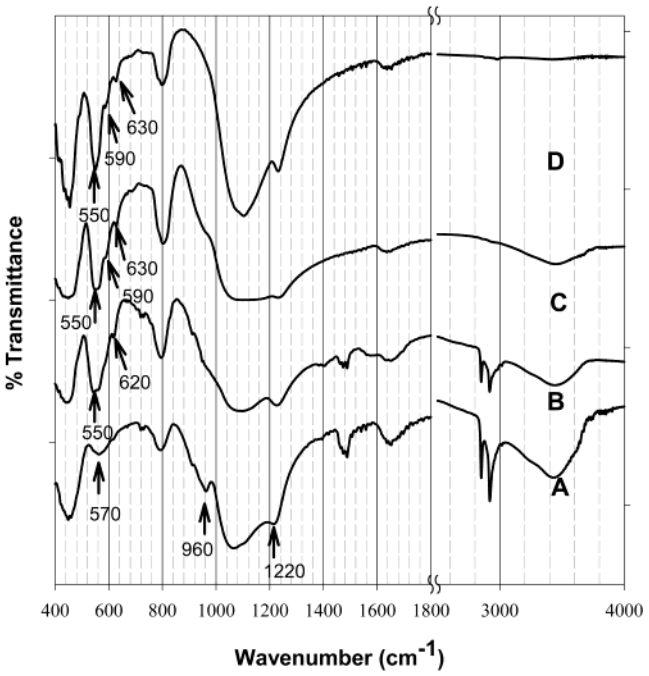

Figure 2. FTIR spectra of (A) NPs collected from the reaction sol after the induction period, (B) nanocrystals produced after steaming, (C) calcined nanocrystals, and (D) calcined reference colloidal silicalite-1 produced from the same recipe.

NPs in the sample.[21] While our XRD pattern is consistent with the presence of nanometer-sized MFI crystallites, it cannot be used to *prove* that MFI crystallites were present in the sample. Several reports contain weak suggestions of this band of peaks,[20,22] but not as prominently as when using the isolation technique reported here and previously.[14] In another report[23] the authors only reported XRD patterns at angles below 5° 2θ, well below the range simulated by Schlenker and Peterson[21] on nanometer-sized MFI. To our knowledge, the only other report showing such a prominent XRD band was given by Tosheva et al.[9,10] on resin templated samples with short reaction times. However, they did not report the particle size of those samples. Although they observed several features different from that of amorphous silica on the Raman spectra of these samples, they were rather conservative and interpreted the Raman peaks as the result of "chainlike structural fragments" of silica.

However, the zeolitic nature of the NPs could be confirmed by the absorption near 550 cm^{-1} in the FTIR spectrum shown in Figure 2A, assigned to the asymmetric stretching mode in the five-membered rings.[19,24] It was shown recently that the peak occurs at 570 cm^{-1} for the nanometer-sized crystallites and shifts to 550 cm^{-1} for larger MFI crystals,[27] exactly as observed in Figure 2. Therefore, the collected NPs were indeed zeolitic pseudocrystalline as reported earlier.[19,26,27]

In addition to this zeolitic ≈570-cm^{-1} absorption, the peaks at 457 and 800 cm^{-1} observed in this spectrum correspond to Si−O−Si rocking and symmetric stretching and bending, respectively. The absorption at 1220 cm^{-1} is the result of Si−O−Si asymmetric stretching.[28] The peak at 960 cm^{-1} is assigned to Q3 silanol groups by Ravishankar et al.[29] This peak is usually more pronounced in TS-1 zeolite and has been taken as an indication of the presence of the Si−O−Ti bond.[28] Since we had no titanium in our system, the assignment to silanol group seemed to be more appropriate.

TPA−Silicalite-1 Nanocrystals Produced after Steaming. Upon steaming, condensation of NPs into nanocrystals, or zeolitization, occurred. This can be seen from the appearance of MFI peaks in the XRD pattern in Figure 1B, and from the enhancement and splitting of the 550−570-cm^{-1} peak in the spectrum in Figure 2B. A small peak at ≈620 cm^{-1} now appears in the FTIR spectrum. All of the above features were suggested as fingerprints for a silicalite nanophase.[29] In addition, the Si−OH absorption at 970 cm^{-1} was significantly reduced, suggesting the consumption of hydroxyl groups during zeolitization.

The pseudocrystalline nature of the NPs in the synthesis of MFI zeolite may not be accidental. Taulelle[30] observed similar results in the earlier stages of $AlPO_4$-JC2 synthesis. A "clipping" process was proposed for the later transformation of these pseudocrystalline nanoprecursors into a proper zeolite crystal. In a broader perspective, Penn et al.[31] recently demonstrated that the solution-phase synthesis of many metal oxides (TiO_2, Fe_2O_3, FeOOH) occur via formation of pseudocrystalline primary units in the first stage. The primary units may aggregate epitaxially and turn into larger crystallites directly, or they may aggregate randomly and produce large crystals after reorientation, recrystallization, and phase transformation.

In our case, the NPs were covered by the surfactant during the flocculation step. This, and the limited amount of water present during the steaming step, facilitated the local zeolitization. This change occurred due to either conversion of residual amorphous silica and TPA to crystalline domains, or linkage of the NPs by a surface condensation process. It is important to note that the amount of water present during steaming is crucial and controls the extent of long-range transport and coarsening processes that may lead to bonded aggregation of the zeolites. Hard aggregates of nanosized zeolites formed when steaming was carried out under saturated water vapor.

Calcined Silicalite-1 Nanocrystals. The nanocrystals produced were stable to the high-temperature

(22) Burkett, S. L.; Davis, M. E. *J. Phys. Chem.* **1994**, *98*, 4647−4653.
(23) Ravishanker, R.; Kirschhock, C. E. A.; Knops-Gerrits, P.-P.; Feijen, E. J. P.; Grobet, P. J.; Vanoppen, P.; de Schryver, F. C.; Miehi, G.; Fuess, H.; Schoeman, B. J.; Jacobs, P. A.; Martens, J. A. *J. Phys. Chem. B* **1999**, *103*, 4960−4964.
(24) Coudurier, G.; Naccache, C.; Vedrine, J. C. *Chem. Commun.* **1982**, *24*, 1413−1415.
(25) Jansen, J. C.; van der Gaag, F. J.; van Bekkum, H. *Zeolites* **1984**, *4*, 369−372.
(26) Chen, S. S.; Chen, Y. W.; Chiang, A. S. T. *Proceedings of Pacific Basen Conference on Adsorption Science & Technology*; Do, D. D., Ed.; World Scientific Inc.: Australia, 2000; pp 130−135.
(27) Kirschhock, C. E. A.; Ravishanker, R.; Verspeurt, F.; Grobet, P. J.; Jacobs, P. A.; Martens, J. A. *J. Phys. Chem. B* **1999**, *103*, 4965−4971.
(28) Armaroli, T.; Milella, F.; Notari, B.; Willey, R. J.; Busca, G. *Top. Catal.* **2001**, *15* (1), 63−71.
(29) Ravishankar, R.; Kirschhock, C.; Schoeman, B. J.; Vanoppen, P.; Grobet, P. J.; Storck, S.; Maier, W. F.; Martens, J. A.; Deschryver, F. C.; Jacobs, P. A. *J. Phys. Chem. B* **1998**, *102* (15), 2633−2639.
(30) Taulelle, F. *Solid State Sci* **2001**, *3* (7), 795−800.
(31) Penn, R. L.; Oskam, G.; Strathmann, G. J.; Searson, P. C.; Stone, A. T.; Veblen, D. R. *J. Phys. Chem. B* **2001**, *105* (11), 2177−2182.

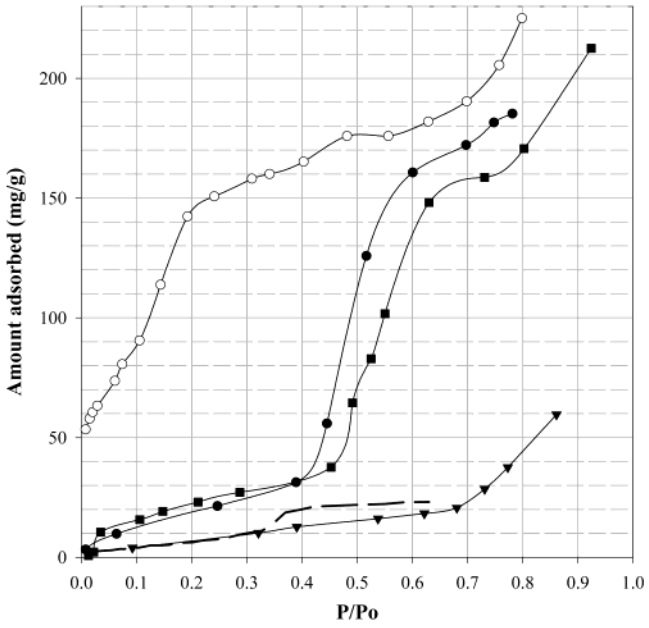

Figure 3. Room-temperature adsorption isotherms of water (solid symbols) and *n*-hexane (open symbol). ● and ■ are repeated runs for calcined nanocrystals. ▲ is for calcined reference colloidal silicalite-1. − − − is the water adsorption isotherm of high silica H−ZSM-5 re-plotted from Olson et al.[33]

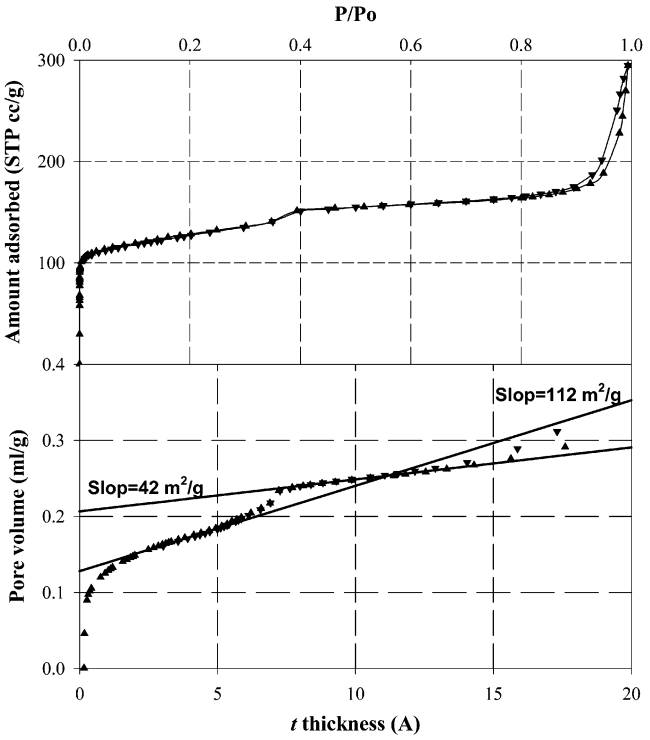

Figure 4. Nitrogen adsorption isotherm (77.3 K) and t-plot analysis based on the reference isotherm of Jaroniec et al.[34]

calcination procedure described in the Experimental Section. The crystallite domain size estimated by applying the Scherrer equation to the 133 peak in the XRD increased from 37 to 39 nm during calcination. The change of crystallite domain size was from 14 to 40 nm when calculated based on the 101 peak. However, the estimated crystallite domain size is always larger than the crystal size observed in TEM.

After calcination, no organic species could be found in the FTIR spectrum, confirming the complete removal of CTAMeBr and TPAOH during calcination. The Si−OH absorption at 970 cm^{-1} practically vanished, and the broad band around 3400 cm^{-1}, which appeared before steaming and calcination, was drastically reduced. It is worth noting that the relative intensity of the 3400-cm^{-1} band for adsorbed water was practically the same as that of the calcined reference colloidal silicalite-1 sample and was much weaker than that of the silicalite-1 nanocrystals synthesized by Corckey and Ninham[32] at room temperature. This suggested that our nanocrystals were similar to colloidal silicalite-1 in water adsorption capacity and may be more hydrophobic than the sample of Corckey and Ninham, as will be proved by the following adsorption studies.

The 25 °C adsorption isotherms for water and *n*-hexane of our nanocrystal and reference colloidal silicalite-1 samples are given in Figure 3, where one water adsorption isotherm was repeated to confirm the results. Also shown in this figure as a dashed line is the water adsorption isotherm reported by Olson et al.[33] on their H−ZSM-5 sample with $SiO_2/Al_2O_3 > 8000$.

Clearly, our colloidal silicalite-1 sample behaved very similar to the micrometer-sized sample of Olson et al. at water vapor pressures below $P/P_o = 0.3$. Above this pressure, Olson's sample showed a step increase of water adsorption, which they suggested might be related to the adsorption at framework defects. Our colloidal sample did not produce such a step until $P/P_o \sim 0.7$. If their suggestion was correct, our colloidal silicalite could have fewer defects.

Compared to the colloidal silicalite-1, the calcined nanocrystals adsorbed more water in the low-pressure range. Furthermore, a huge amount of condensation occurred above $P/P_o = 0.4$. The saturation water capacity of the nanocrystal was about 185 mg/g, which is the expected pore-filling value for water in silicalite-1. For *n*-hexane, the first point of adsorption at very low pressure was already 50 mg/g, which is typical for micropore adsorption. The isotherm then increased linearly until $P/P_o \sim 0.2$ and changed slope afterward. According to the suggestion of Olson et al.,[33] one can use the water to *n*-hexane adsorption ratio at $P/P_o \sim 0.04$ or 0.25 as a measure of hydrophobicity. The data on our nanocrystals led to 92% and 84% hydrophobicity, respectively, at these two pressure ratios. This compared favorably to their values in the range of 75−99% over a range of Si/Al values.[33]

The calcined nanocrystals were further characterized by nitrogen adsorption at 77.3 K. The isotherm is shown in Figure 4A, where a small step at $P/P_o \sim 0.4$ and a larger step increase after $P/P_o = 0.9$ were observed. The steep rise at $P/P_o = 0.9$ was related to the texture porosity and suggested that the sample consisted of mainly 100−200-nm-sized powders. The small step at $P/P_o \sim 0.4$ was the result of condensation in the intercrystalline mesopores. The BET surface area of the sample was found to be 440 m^2/g when the usual range of $P/P_o = 0.05-0.2$ data were fitted. It became 470 m^2/g if data in the $P/P_o = 0.005-0.1$ range was used. The

(32) Corkery, R. W.; Ninham, B. W. *Zeolites* **1997**, *18*(5−6), 379−386.

(33) Olson, D. H.; Haag, W. O.; Borghard, W. S. *Microporous Mesoporous Mater.* **2000**, *35*−*36*, 435−446.

standard BJH pore size analysis supplied by the instrument suggested that there were about 0.05 cm^3/g of intercrystalline mesopores narrowly distributed around 3 nm, consistent with the estimated size of the nanocrystals. The HK analysis suggested that there were about 0.1 cm^3/g of micropores in ≈5A size range, also consistent with the zeolitic nature of the nanocrystals.

The t-plot method was used to separate the specific pore volume of intercrystalline voids and micropores as shown in Figure 4B. The relative pressure was first converted to the t-thickness using the reference isotherm reported by Jaroniec et al.[34] The linear fit of the data between $t = 2$ and $t = 5$ Å gave the micropore volume, 0.128 cm^3/g, as the intersection and a slope of 112 m^2/g. This can be used as an estimate of the external surface area of the nanocrystals. Another linear section appeared for data following the step change at $P/P_o = 0.4$. The straight line fitted from this section gave the combined volume of 0.206 cm^3/g for meso- and micropores. The slope of this section, 42 m^2/g, is then the surface area of the texture porosity when the intercrystalline voids were filled with nitrogen.

Had we calculated the t thickness according to the classical Harkins and Jura or Halsey relations, the external surface area would be 215 and 226 m^2/g, respectively. The micropore volume would be 0.11 and 0.08 cm^3/g, respectively, with the combined meso- and micropore volume remaining as 0.21 cm^3/g. It is known that the two classical relations can only be applied for P/P_o above 0.1, whereas the reference isotherm given by Jaroniec et al. was measured down to $P/P_o = 10^{-5}$. Furthermore, a t-plot constructed from the classical relations always leads to a negative intersect for MCM-41 type of materials, whereas that based on Jaroniec et al. reference isotherm predicts zero micropore volume. Therefore, before the differences on t-thickness is resolved, it is safer to claim that the external surface area of our nanocrystals is >112 m^2/g.

In any case, the external surface area obtained from our sample is comparable to that of the zeolitic nanocrystals synthesized in the earlier works,[32,35] whereas the micropore volume is 60% of that observed in micrometer-sized crystals. If one assumes that the outermost layer of one unit cell depth (≈1-nm thick) does not contribute to the micropore volume, the reduction of micropore volume for a 20-nm crystal would be about 33%, in reasonable agreement with our findings.

Camblor et al.[36] recently demonstrated the dependence of zeolite micropore volume on crystal sizes. They predicted a micropore volume of ≈0.12 cm^3/g for zeolite crystals of 10−20-nm sizes, which is in agreement with the results obtained on our nanocrystals.

Dispersion of Calcined Silicalite-1 Nanocrystals. Fifty milligrams of the calcined nanocrystals was placed in a 15-mL glass vial with 5 mL of ethanol and 2 mL of 20% ammonia and subjected to ultrasonication in a Bransen 3510 ultrasonic bath at 40 kHz for 3 h. The temperature increased to 60 °C during the treatment. The solution after the ultrasonication treatment appeared clear; however, closer examination revealed the presence of tiny entities that deflected light at the air−liquid interface. A sample was prepared for TEM analysis by placing a drop of diluted clear solution on a carbon-coated copper grid. Two types of morphologies were observed under TEM. The first consisted of well-formed square-shaped nanocrystals 10−20 nm in size (Figure 5A), whereas the other existed in the form of hollow spheres of about 100−300-nm size. From Figure 5B to 5D it is clear that the shell of the hollow spheres is about 20 nm in thickness and is made up of nanocrystals.

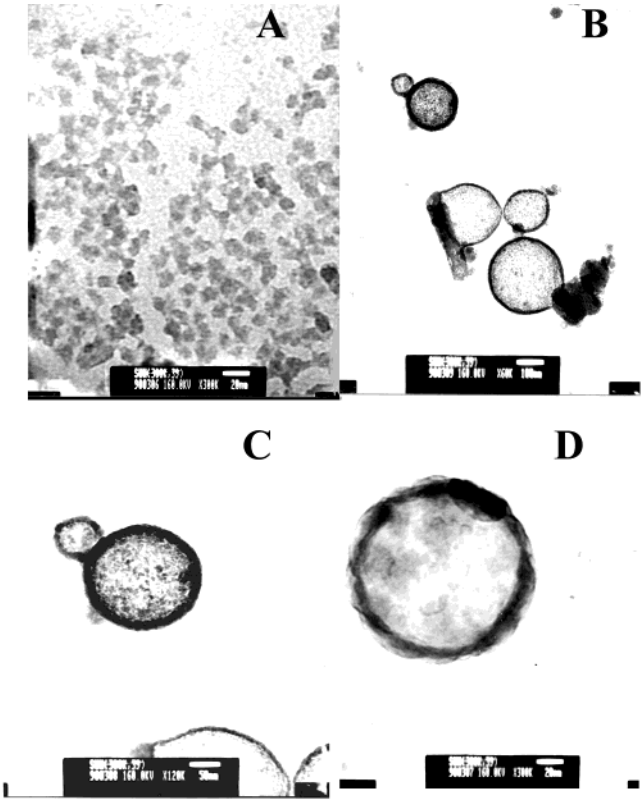

Figure 5. TEM photographs of (A) dispersed nanocrystals. (B)−(D) hollow spheres observed under different magnifications.

It is known that the ultrasonic treatment of a solution creates acoustic cavitation.[37] Small pockets of gas and vapor (cavitation bubbles) of various sizes exist in liquids. The cavitation bubbles grow and collapse violently under the influence of the rarefaction and compression pressure cycles of ultrasound. Collapsing cavities attain high temperatures and pressures. Because of the hydrophobic nature of silicalite-1 nanocrystals, it was expected that they would gather around the cavitation bubbles and fuse into hollow spheres under the high temperature created by the collapse of these cavities. Similar fusion of 150-nm nanocrystals by ultrasonication has also been observed in the case of zeolites A and X,[8] where surfactant was used to disperse them in a toluene/water mixture.

As of now, the exact mechanism for the formation of the hollow spheres requires more study. However, their mere presence suggests that the direct ultrasonication

(34) Jaroniec, M.; Kruk, M.; Olivier, J. P. *Langmuir* **1999**, *15*, 5410−5413.
(35) Schmidt, I.; Madsen, C.; Jacobsen, C. J. H. *Inorg. Chem.* **2000**, *39* (11), 2279−2283.
(36) Camblor, M. A.; Corma, A.; Valencia, S. *Microporous Mesoporous Mater.* **1998**, *25* (1−3), 59−74.
(37) Suslick, K. S.; Didenko, Y.; Fang, M. M.; Hyeon, T.; Kolbeck, K.; McNamara, W. B.; Mdleleni, M. M.; Wong, M. *Philos. Trans. R. Soc. London A* **1999**, *357*, 335−353.

may be an easier way to form hollow spheres with zeolitic shells compared to the surfactant-stabilized microemulsion approach used by Kulak et al.[8]

Conclusions

Nanocrystals of silicalite of size ≈10−20 nm with >112 m^2/g of external surface were prepared via the steaming of isolated nanoprecursors. The nanocrystals were somewhat hydrophobic in nature. The dispersion of these nanocrystals under ultrasound produced hollow spheres with a shell of fused nanocrystals. The method of nanocrystal synthesis, as well as the formation of hollow spheres, appears to be a general one. Further studies are needed for a better understanding of the organization phenomenon observed in the sonication of the nanozeolite crystals.

Acknowledgment. Support of National Science Council, Republic of China. through Grant NSC-90-2214-E008-008 is acknowledged. S.P.N. thanks NSC for a postdoctoral fellowship.

CM020786V